Progress in the peeling-ballooning model of edge localized modes: Numerical studies of nonlinear dynamics[a)]

P. B. Snyder[b)]
General Atomics, P.O. Box 85608, San Diego, California 92186-5608

H. R. Wilson
EURATOM/UKAEA Culham Science Centre, Abingdon, Oxon OX1 3DB, United Kingdom

X. Q. Xu
Lawrence Livermore National Laboratory, Livermore, California 94550

(Received 12 November 2004; accepted 2 December 2004; published online 22 April 2005)

Nonlinear three-dimensional electromagnetic simulations are employed to study the dynamics of edge localized modes (ELMs) driven by intermediate wavelength peeling-ballooning modes. It is found that the early behavior of the modes is similar to expectations from linear, ideal peeling-ballooning mode theory, with the modes growing linearly at a fraction of the Alfvén frequency. In the nonlinear phase, the modes grow explosively, forming a number of extended filaments which propagate rapidly from the outer closed flux region into the open flux region toward the outboard wall. Similarities to nonlinear ballooning theory as well as additional complexities are observed. Comparison to observations reveals a number of similarities. Implications of the simulations and proposals for the dynamics of the full ELM crash are discussed. © *2005 American Institute of Physics*. [DOI: 10.1063/1.1873792]

I. INTRODUCTION

Understanding the physics of the *H*-Mode pedestal and edge localized modes (ELMs) is very important to next-step magnetic fusion devices for two primary reasons: (1) the pressure at the top of the edge barrier (pedestal height) strongly impacts global confinement and fusion performance, and (2) large ELMs lead to localized transient heat loads on material surfaces that may constrain component lifetimes. The development of the peeling-ballooning model has shed light on these issues by positing a mechanism for ELM onset and constraints on the pedestal height. The mechanism involves instability of ideal coupled "peeling-ballooning" modes driven by the sharp pressure gradient and consequent large bootstrap current in the *H*-mode edge. It was first investigated in the local, high-n limit,[1] and later quantified for nonlocal, finite-n modes in general toroidal geometry.[2,3] Important aspects are that a range of wavelengths may potentially be unstable, with intermediate n's ($n \sim 3-30$) generally limiting in high performance regimes, and that stability bounds are strongly sensitive to shape [Fig. 1(a)], and to collisionality (i.e., temperature and density) (Ref. 4) through the bootstrap current. The development of efficient magnetohydrodynamic (MHD) stability codes such as ELITE (Refs. 3 and 2) and MISHKA (Ref. 5) has allowed detailed quantification of peeling-ballooning stability bounds [e.g., Ref. 6] and extensive and largely successful comparisons with observation [e.g., Refs. 2 and 6–9]. A typical peeling-ballooning mode structure, calculated with ELITE for toroidal mode number n of 18, is shown in Fig. 1(b). This $n=18$ mode is found to be approximately the most unstable in this DIII-D tokamak discharge at a time immediately before an ELM is observed. The mode consists of a series of filaments of positive and negative amplitude [positive amplitude filaments are shown in Fig. 1(b)] which grow in the outer (typically 4%–15%) part of the closed flux region of the plasma. The mode has a characteristic ballooning structure, with largest amplitude on the outboard "bad curvature" side, and very small amplitude on the inboard side.

Previous peeling-ballooning studies have been largely ideal and linear, focusing on the onset conditions of the modes and their structure in the early linear phase. Here we extend this work to incorporate the impact of nonideal, nonlinear dynamics, investigating the evolution of these modes into the strongly nonlinear state, and allowing study of the transport of particles and heat from the closed flux region to the open field-line scrape-off layer (SOL), and ultimately material surfaces. In Sec. II the methods and results of the nonlinear simulations are discussed, and these results are compared with experimental observations in Sec. III. Section IV presents a discussion of proposed mechanisms for the transport of particles and heat during the full ELM crash, as well as concluding remarks and a brief discussion of future work.

II. NONLINEAR SIMULATIONS

While linear stability studies have proved quite useful for understanding ELM onset and pedestal constraints, quantitative prediction of ELM size and heat deposition on material surfaces requires nonlinear dynamical studies. Nonlinear *H*-mode edge physics studies are in general quite challenging, due to the very wide range of relevant spatiotemporal

[a)]Paper JI2 5, Bull. Am. Phys. Soc. **49**, 209 (2004).
[b)]Invited Speaker.

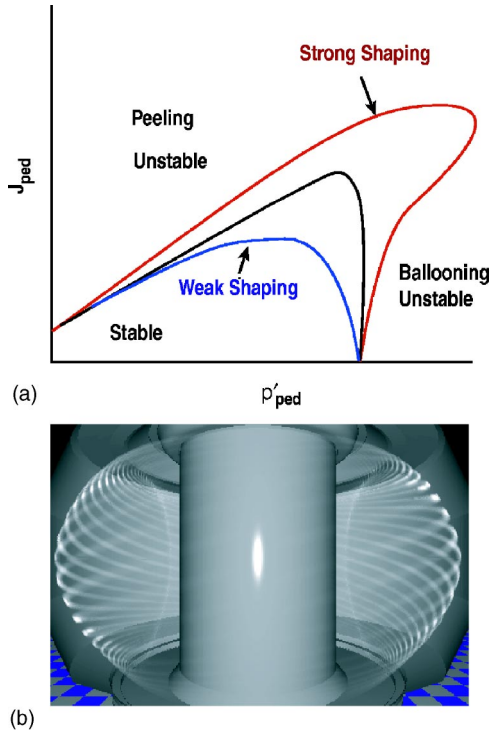

FIG. 1. (a) Schematic diagram of peeling-ballooning stability bounds vs edge current and pressure gradient for different shaped equilibria. (b) Mode structure calculated by ELITE of an $n=18$ peeling-ballooning mode in DIII-D discharge 119 049. Rendered in 3D with intensity proportional to the line integral of positive perturbation strength along the line of sight.

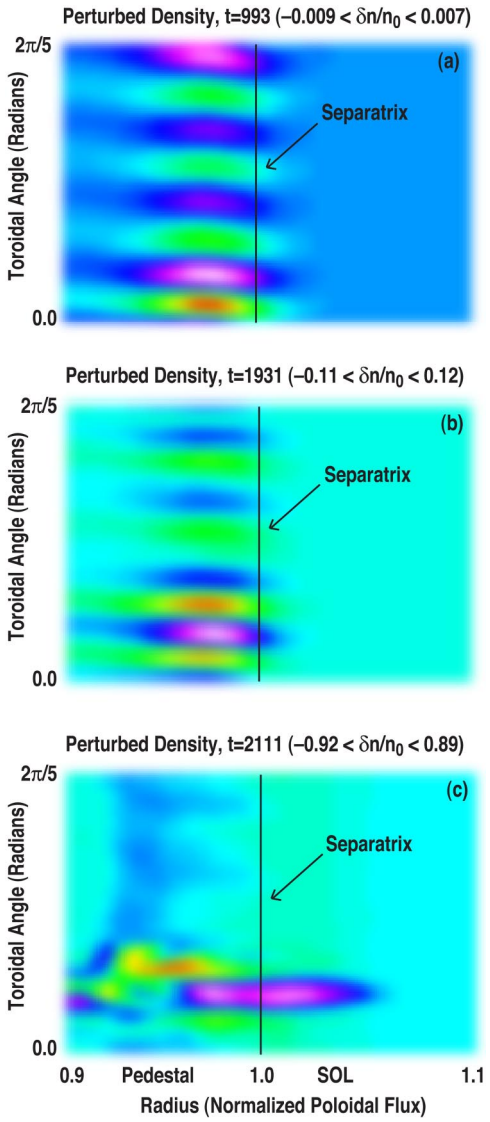

FIG. 2. Contour plots of the normalized density perturbation ($\delta n/n_0$) along the outer midplane at early times (a) shows the expected peeling-ballooning structure (here $n=20$) in the pedestal region. Later (b) a more pronounced toroidal localization is seen, followed by (c) a fast radial burst across the separatrix, localized toroidally, but extended along the field.

scales, and the breakdown of a number of approximations (e.g., small perturbations, locality) that have simplified core plasma simulations. Here we address this challenge via a focus on the scales of the fast ELM crash event itself, initializing simulations with peeling-ballooning unstable equilibria and following the mode dynamics into the strongly nonlinear phase. We employ the three-dimensional (3D) reduced Braginskii BOUT code,[10,11] modified to include the equilibrium kink/peeling drive term.[11] BOUT employs field-line-following coordinates for efficiency, and simulates the pedestal and SOL regions (typically $0.9<\Psi_N<1.10$, where Ψ_N is the normalized poloidal flux). Because the coordinates are field aligned (quasiballooning, though radially nonlocal) it is not in general necessary to simulate the full toroidal domain when studying modes whose toroidal correlation lengths are relatively small. Here we employ a $1/5$ toroidal domain ($\Delta n=5, n=0,5,10,\ldots,160$), which allows resolution of length scales of order the ion gyroradius ρ_i where diamagnetic and finite-Larmor-radius physics produces a natural cutoff of small scales. The full (2π) poloidal domain is simulated, including the private flux region. A zero potential boundary condition is imposed on the outer radial boundary ($\Psi_N=1.1$), and a zero gradient boundary condition is imposed on the inner boundary ($\Psi_N=0.9$).

We study a typical DIII-D high density H-mode discharge, with toroidal field $B_T=1.5$ T, plasma current $I_p=1.15$ MA, and pedestal density $n_{e,ped}=7.6\times10^{13}$ cm^{-3}. The discharge exhibits what are known as "small Type I" ELMs, and the initial equilibrium is constructed from measured profiles just before an ELM is observed. The initial equilibrium is found by ELITE to be linearly unstable, with substantial growth rate, to a range of intermediate to high n modes. Nonlinear BOUT simulations are initialized with this equilibrium, and evolved into the strongly nonlinear phase, with results given in Figs. 2–4. In the early stage of the simulation, a fast growing mode is seen in the sharp gradient region of the pedestal, with approximately the growth rate and spatial structure expected from linear peeling ballooning calculations. The dominant mode in the linear phase is $n=20$, as shown in Fig. 2(a) (note again that $\Delta n=5$ is used, hence what appears as $n=4$ in the $1/5$ toroidal domain is an $n=20$ mode), with a growth rate $\gamma/\omega_A\sim0.15$, where ω_A is the Alfvén frequency. At later times, ($t>\sim2000$, where t is normalized by the ion cyclotron frequency $\Omega=5.65\times10^7$ s^{-1}) a very rapid burst occurs resulting in the expulsion of particles and heat across the separatrix, in a filamentary structure that

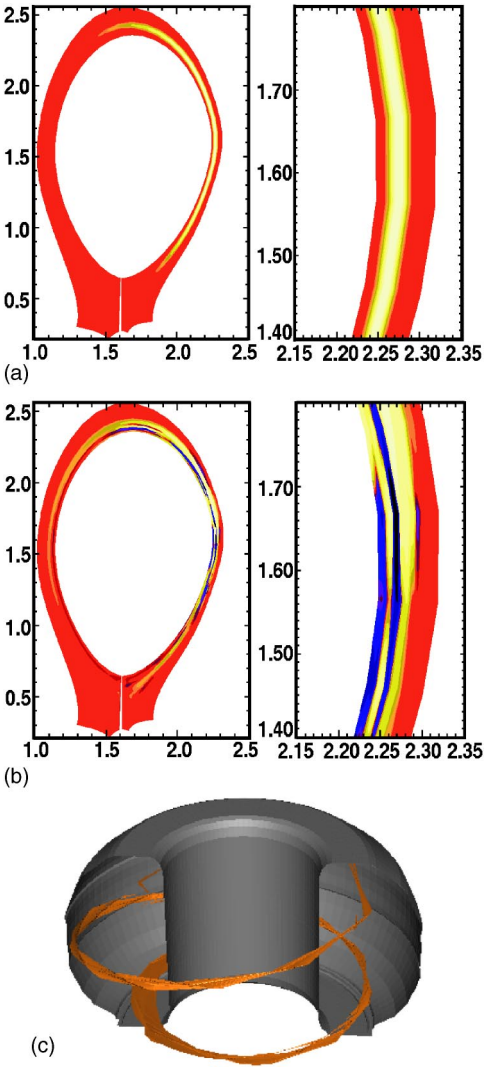

FIG. 3. Contours of the perturbed density as a function of radial and poloidal coordinates at (a) $t=100$ and (b) $t=2105$. The poloidal coordinate extends in and out of the page along the magnetic field, but a flat projection is shown. The mode shows the expected ballooning structure at early times (a), with maximum amplitude near the outboard midplane, and maintains a similar though more complex poloidal structure during the radial burst phase (b). (c) Shows a surface of constant perturbed density at the late time ($t=2106$), rendered in 3D to show the structure of the radially propagating filament.

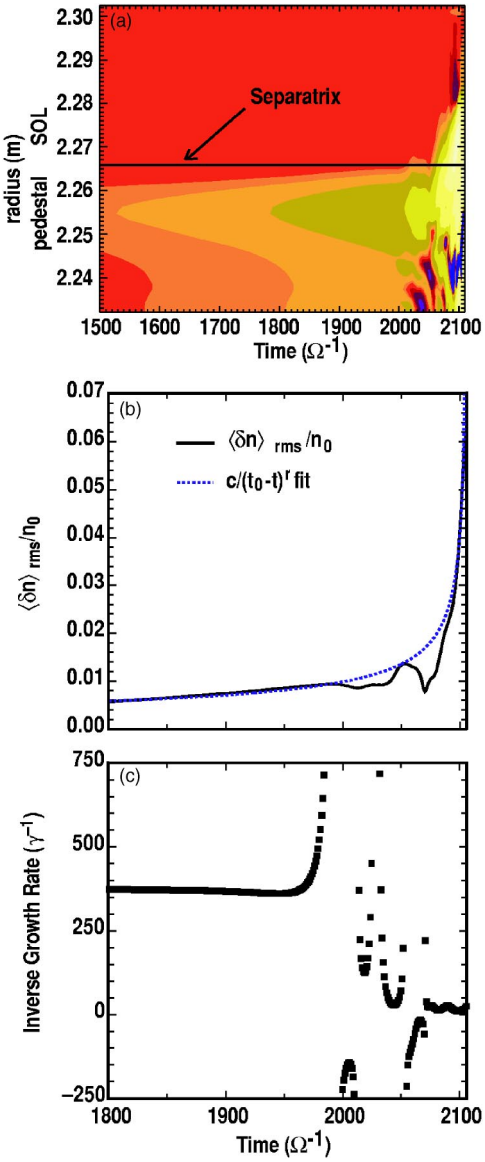

FIG. 4. (a) Contour plot of the evolution of the perturbed density on the outboard midplane. (b) Evolution of the rms density perturbation at the separatrix, compared to a fit of the form $1/(t_0-t)^r$. (c) Inverse growth rate of the perturbed density as a function of time.

is radially extended, but localized in the cross field (toroidal) direction as shown in Fig. 2(c). Figures 3(a) and 3(b) show the poloidal structure of the mode, which maintains a characteristic ballooning structure, with maximum amplitude near the outboard midplane, and very small amplitude on the inboard (high field) side. Figure 3(c) shows the 3D structure of the radial burst in the explosive nonlinear phase. The mode evolves into a filament extended along the magnetic field across the outboard side of the torus as it propagates outward. We note that this fast growing, nonlinear bursting mode does appear to be consistent with the basic peeling-ballooning model, as the mode does not exist when parameters are lowered significantly below the linear peeling-ballooning threshold. We also note that because the simulations are initialized with significantly supercritical values of the gradients, they may produce faster evolution of the mode than expected in experiment, where gradients are generally pushed across the critical point on the relatively slow transport time scale.

Several characteristics of the early nonlinear phase of the simulations are qualitatively consistent with predictions of nonlinear ballooning theory.[12] The theory posits that the dominant nonlinear terms weaken the stabilizing effects of field-line bending, resulting in a growth rate that increases with time during the early nonlinear phase (explosive growth), and fast radial propagation of extended filaments. A simplified version of the theory predicts perturbations growing as $1/(t_0-t)^r$ toward a finite time singularity at $t=t_0$. Figure 4(a) shows the time evolution of the perturbed density as a function of radius on the outboard midplane, with approximately linear growth of the mode in the sharp gradient region of the pedestal at early times, followed by a fast radial burst at $t > \sim 2000$. The evolution of the perturbed density in

the simulations is complex [Fig. 4(a) and 4(b)], punctuated by temporary decreases in amplitude before the final rapid burst. However, the overall structure fits well with the explosive form $c/(t_0-t)^r$, as shown by the dashed line in Fig. 4(b), fit with $r=1/2$. Note that this value of $r=1/2$ differs quantitatively from the value expected from nonlinear ballooning theory ($r=\sqrt{1-4D_M}\approx 1.1$),[12] though the qualitative trend of explosive growth is similar. The growth rate $1/\delta n\, d(\delta n)/dt$, calculated from a seven point boxcar average, generally shows the expected explosive behavior [Fig. 4(c)], with growth rate increasing slowly with time at early times, and then a trend toward a very fast increase during the late phase of the simulations (broken up by occasional lulls). The emergence of complex behavior in the simulations at $t\sim 2000$ corresponds roughly to the time at which the perturbed quantities ($\delta n/n_0$, $e\varphi/T_0$, etc.) become order 1, and to the time at which the local perturbed density becomes comparable to the total density at outer locations, breaking the symmetry between positive and negative δn.

An important question not addressed by nonlinear ballooning theory is whether one or several propagating filaments are expected in the explosive nonlinear phase. In the simulation shown in Figs. 2–4 a single dominant filament emerges at a particular toroidal location in the simulation domain. In this simulation, a broad band of toroidal mode numbers are initialized at random phase. Analysis of the time evolution of the spectrum reveals that multiple modes grow linearly, with nonlinear coupling of nearest neighbors driving the lowest n in the box ($n=5$ in this $\Delta n=5$ simulation) strongly. It is then the point of maximum resonance between the dominant linear mode ($n=20$) and this strongly nonlinearly driven mode ($n=5$) that determines the toroidal location of the maximum perturbation amplitude [white region in Fig. 2(b)], where the fast radial propagating burst occurs [Fig. 2(c)]. Note that while this simulation was carried out in a $\Delta n=5$ box, the result can be extrapolated to a full torus ($\Delta n=1$) box, where nearest neighbor linear modes will beat together to drive an $n=1$ mode, which will then determine a toroidal location of maximum resonance. This mechanism of course requires multiple unstable linear modes. If the same simulation is carried out, initialized with only a pure $n=20$ mode, the result is quite different, as shown in Fig. 5. Even in the strongly nonlinear phase [Fig. 5(b)], only harmonics ($n=0,20,40,80,120$) are present at significant amplitude, and the radial burst [Fig. 5(c)] occurs with approximate symmetry, with a full contingent of 20 filaments propagating radially into the SOL. In general, both the single filament (Fig. 2) and multiple filament (Fig. 5) cases are physically realizable, depending upon the flatness of the growth rate spectrum, and the rate at which the edge profiles are driven across the marginal point.

We note evidence of secondary instabilities breaking up the radial structure of the mode in Fig. 5(b) and 5(c) as well as Fig. 2(c). The origin and evolution of these secondary instabilities, including comparisons to the existing "blob" formation and evolution literature [e.g., Refs. 13–15], are an important topic for future study.

We have focused on a set of simulations using a single initial equilibrium for simplicity of the discussion, but note

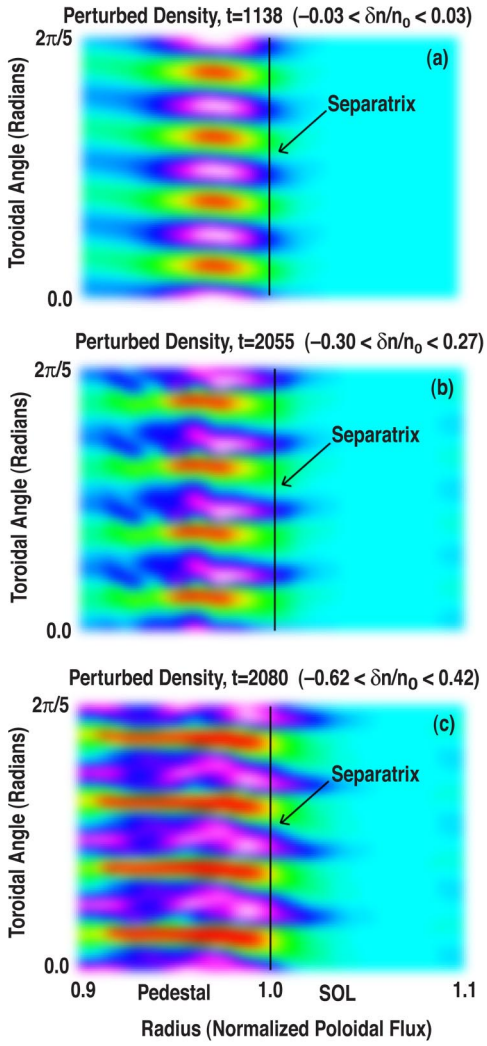

FIG. 5. Contour plots of the normalized density perturbation ($\delta n/n_0$) along the outer midplane, from a simulation initialized with a single toroidal mode ($n=20$). (a) Shows the expected peeling-ballooning structure ($n=20$) in the pedestal region during the linear phase. At later times (b) and (c) the mode remains approximately toroidally periodic, even as the simulation becomes strongly nonlinear, and filaments burst radially outward.

that the general characteristics described above: (1) a linear growth phase with mode characteristics similar to those expected from linear peeling-ballooning studies, (2) a brief lull in the growth rate near the time where $\delta n/n_0\sim 1$ locally, and (3) explosive growth of one or many filaments, and fast radial propagation into the SOL, appear to be generic characteristics of several cases studied thus far.

III. COMPARISON TO EXPERIMENT

Filamentary structures associated with ELM onset have been observed on multiple tokamaks. An observation [Figs. 6(a) and 6(b)], using data from a poloidal array of fast magnetic probes on the DIII-D tokamak,[16] found that the ELM magnetic perturbation [Fig. 6(a)] is associated with a single filamentary structure extended along the outboard (low field) side. For comparison, we have plotted the BOUT simulation results from Figs. 2–4 at a late time ($t=2106$) during the nonlinear burst phase as a function of poloidal and toroidal

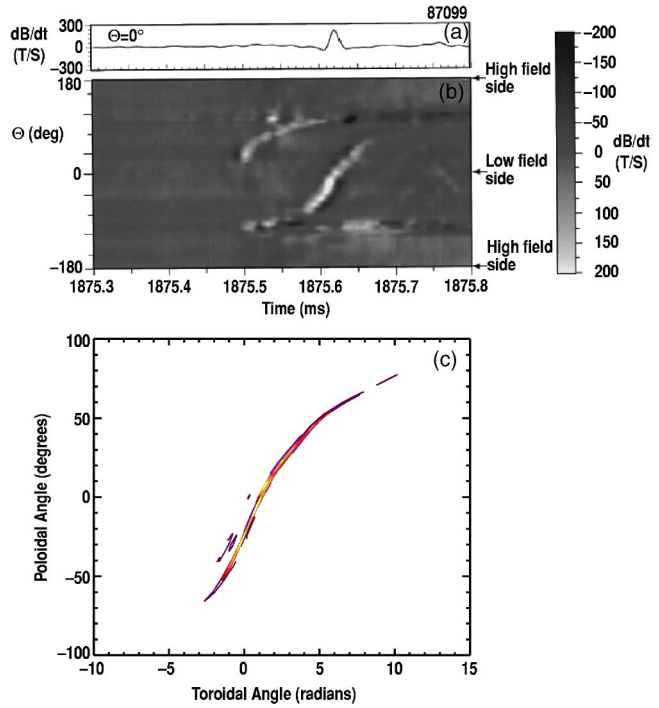

FIG. 6. Measured time and poloidal angle dependencies of an edge instability in the DIII-D tokamak: (a) time evolution of dB/dt from a magnetic probe on the outer midplane, and (b) contour plot of dB/dt vs time and poloidal angle. This is compared to (c) a contour plot of the perturbed density from BOUT simulation results (from the case shown in Figs. 2–4) at $t=2106$, in poloidal vs toroidal angle space. The time axis in (b) can be mapped to toroidal angle using the observed toroidal rotation speed of the mode.

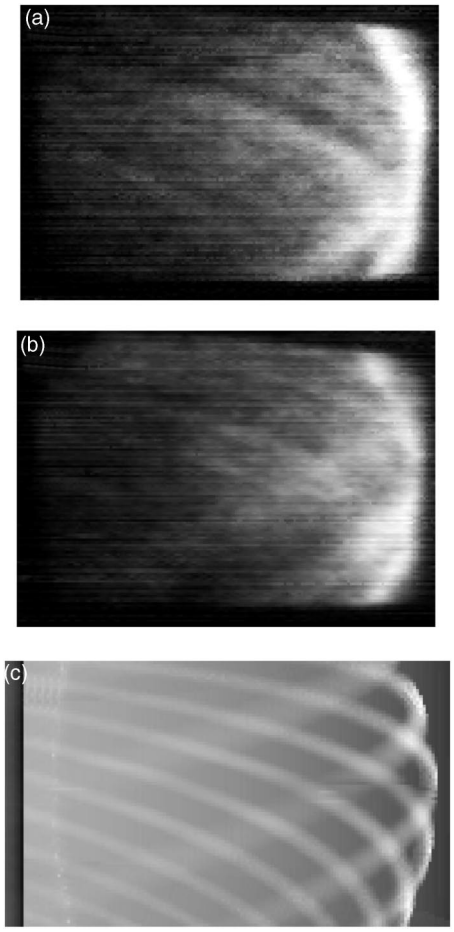

FIG. 7. CIII images during ELM events for two DIII-D discharges (a) and (b). (c) Mode structure calculated by ELITE for an $n=18$ peeling-ballooning mode in an equilibrium reconstructed using measured profiles just prior to the ELM event observed in (b).

angle in Fig. 6(c). Because the mode is rotating toroidally in the experiment (as expected from peeling-ballooning theory with rotation[17]), time can be mapped to toroidal angle. The general characteristics of the observed filament, including its poloidal extent and filamentary structure, are quite similar to the simulation results. Similar observations of filamentary structures during ELMs in magnetic probe data have been made on the COMPASS tokamak.[18]

Filaments associated with ELM onset have also been directly observed using fast (few microsecond exposure) cameras. Multiple images from the Mega Amp Spherical Tokamak (MAST) spherical tokamak[19] clearly show a set of filaments associated with the ELM event, with a relatively symmetric structure ($n\sim10$). Recent observations[20] of CIII emission during the ELM event on the DIII-D tokamak similarly show a filamentary structure, as shown in Figs. 7(a) and 7(b). Estimates based on the spacing between filaments suggest a mode number of approximately $n\sim18$. For the case shown in Fig. 7(b) (DIII-D shot 199 449), an equilibrium has been reconstructed using profiles measured shortly before the observed ELM. Using ELITE, this equilibrium is found to be marginally unstable, with the most unstable mode number falling in the range $15<n<25$; that is, the first mode to go significantly unstable is expected to fall within this range of mode numbers. The mode structure calculated by ELITE for $n=18$ has been rendered in 3D, and is shown in Fig. 1(b). A view of this mode structure similar to the fast camera view is shown in Fig. 7(c). Note that both the apparently broad (because of proximity to the camera) filaments in the near field and the apparently narrow filaments in the far field of the camera are qualitatively similar between the observation [Fig. 7(b)] and the calculated linear mode [Fig. 7(c)]. The observations are expected to correspond to the nonlinear phase of the ELM in which the filaments have radially propagated into the SOL, generating CIII emission, and indeed the observed mode structure shows significant asymmetry. Nonlinear simulations with BOUT have also been carried out for this case. In the early phase of these simulations, the mode structure is symmetric and similar to the linear structure shown in Fig. 7(c). During the explosive nonlinear phase the mode develops a degree of asymmetry, with some filaments growing to significantly larger amplitude than others.

A number of additional measurements on DIII-D, including beam emission spectroscopy and scanning probe data[21] appear to be consistent with filamentary structures propagating at rapid radial velocities during the ELM crash.

IV. DISCUSSION

Nonlinear simulations using the 3D electromagnetic reduced-Braginskii code BOUT have been employed to study the evolution of peeling-ballooning modes thought to be re-

sponsible for edge localized modes in tokamaks. In the early, linear phase of the simulations, mode characteristics, including growth rate and structure, are similar to those expected from linear peeling-ballooning theory. In the later, nonlinear stages, the mode grows explosively, and one or many filaments propagate radially into the open field-line region, carrying particles and heat. Evidence of secondary instabilities breaking up the extended radial filaments is seen in the latter stages of the simulations.

A single dominant filament is expected in the case where the growth rate spectrum is relatively flat, and multiple toroidal mode numbers n are driven linearly unstable before a single (most unstable) n mode grows to large ($\delta n/n_0 \sim 1$) amplitude. In this case, nearest neighbor linear modes couple to nonlinearly drive a low n mode. The location of maximum resonance between the dominant linear mode and the strongly driven nonlinear mode then determines the toroidal location at which the burst occurs. In the case where a single toroidal mode is able to grow to large amplitude before other n values grow to significant amplitude, the instability remains approximately toroidally periodic well into the nonlinear phase, and multiple (approximately n) filaments propagate outward.

Several characteristics of the BOUT simulation results are qualitatively consistent with nonlinear ballooning theory,[12] including explosive growth of the filaments, with perturbations growing roughly as $\sim 1/(t_0-t)^{\mathrm{r}}$, and growth rate increasing with time. Additional complexity is seen in the simulations, including a characteristic lull that occurs in the early nonlinear phase and may be associated with the perturbed density becoming comparable in magnitude to the local equilibrium density in some locations, breaking the symmetry between positive and negative density perturbations.

A number of characteristics of the simulation results, including poloidal extent and filamentary structure, are consistent with fast ELM observations on multiple experimental devices.

We note that these filamentary structures observed in the simulations and in experiment are associated with the ELM event, but that simple loss of the energy and particle content of the (one or many) filaments themselves cannot account for the large losses of particles and heat associated with the full ELM crash. We propose two possible mechanisms to explain these losses. In the first mechanism, proposed in Ref. 12, the filaments act as conduits, which remain connected to the hot core plasma. Fast diffusion and/or secondary instabilities in the outward propagating region of the filament allows loss of particles and heat from the filament to nearby open field-line plasma. The ends of the field line remain connected to the hot core plasma, allowing parallel flow and consequent loss of a substantial amount of heat and/or particles from the core. In the second mechanism, the growth and propagation of the filament causes a collapse of the edge transport barrier, resulting in a temporary return of L-mode-like edge transport, and rapid loss of particles and heat from the edge region. The presence of sheared flow in the edge region weakly suppresses the growth of peeling-ballooning modes,[17] however, once mode growth begins, it proceeds with a single eigenfrequency. As the mode grows and propagates radially, it suppresses the sheared flow in the edge region, via the mode $J \times B$ torque, and, particularly in the case of low n edge modes, coupling to the resistive wall. In the absence of the sheared flow, the edge transport barrier collapses, and strong turbulent transport mechanisms usually associated with L mode return temporarily. As edge profiles relax, the drive of the peeling-ballooning instability is removed, and the flow shear and edge barrier are able to reestablish themselves, and the ELM cycle repeats itself. We note that collapse of the edge E_{r} well has indeed been observed during the ELM crash.[22] It is of course possible that both of the above mechanisms are important in the full ELM event. We note that collisional suppression of electron heat flow along field lines (suppressing the "conduit" mechanism) may explain the observed decrease in conductive heat transport for ELMs in high density plasmas, while the barrier collapse and recovery time might determine the minimum "pure convective" ELM size.

Ongoing studies are focused on extending the duration of the nonlinear simulations to explore the above mechanisms and allow comparisons with experiment across the full ELM duration. Another high priority is extending the spatial extent of the simulations to allow study of the full range of global ($n=1$) through ion gyroradius scales, and eventually conducting transport time scale simulations starting with a stable equilibrium and pushing it slowly across the peeling-ballooning stability threshold.

ACKNOWLEDGMENTS

The authors gratefully acknowledge contributions from Dr. D. P. Brennan, Professor S. C. Cowley, Dr. M. E. Fenstermacher, Dr. A. W. Leonard, Dr. W. Meyer, Dr. T. H. Osborne, Dr. E. J. Strait, Dr. M. Umansky, and the DIII-D Team.

This is a report of work supported by the U.S. Department of Energy under Contract No. DE-FG03-95ER54309 at General Atomics and Contract No. W-7405-ENG-48 at University of California Lawrence Livermore National Laboratory, and supported in part by the United Kingdom Engineering and Physical Sciences Research Council and EURATOM.

[1] J. W. Connor, R. J. Hastie, H. R. Wilson, and R. L. Miller, Phys. Plasmas **5**, 2687 (1998); C. C. Hegna, J. W. Connor, R. J. Hastie, and H. R. Wilson, *ibid.* **3**, 584 (1996).
[2] P. B. Snyder, J. R. Wilson, J. R. Ferron *et al.*, Phys. Plasmas **9**, 2037 (2002).
[3] H. R. Wilson, P. B. Snyder, G. T. A. Huysmans, and R. L. Miller, Phys. Plasmas **9**, 1277 (2002).
[4] P. B. Snyder and H. R. Wilson, Plasma Phys. Controlled Fusion **45**, 1671 (2003).
[5] G. T. A. Huysmans, S. E. Sharapov, A. B. Mikhailovskii, and W. Kerner, Phys. Plasmas **8**, 4292 (2001).
[6] P. B. Snyder, H. R. Wilson, J. R. Ferron *et al.*, Nucl. Fusion **44**, 320 (2004).
[7] D. A. Mossessian, P. Snyder, A. Hubbard, J. W. Hughes, M. Greenwald, B. LaBombard, J. A. Snipes, S. Wolfe, and H. Wilson, Phys. Plasmas **10**, 1720 (2003).
[8] S. Saarelma, S. Günter, L. D. Horton, and ASDEX Upgrade Team, Nucl. Fusion **43**, 262 (2003).
[9] L. L. Lao, Y. Kamada, T. Okawa *et al.*, Nucl. Fusion **41**, 295 (2001).

[10]X. Q. Xu, R. H. Cohen, W. M. Nevins *et al.*, Nucl. Fusion **42**, 21 (2002).
[11]X. Q. Xu, W. M. Nevins, R. H. Cohen, J. R. Myra, and P. B. Snyder, New J. Phys. **4**, 53 (2002).
[12]H. R. Wilson and S. C. Cowley, Phys. Rev. Lett. **92**, 175006 (2004).
[13]D. A. D'Ippolito, J. R. Myra, D. A. Russell, and G. Q. Yu, Phys. Plasmas **11**, 4603 (2004).
[14]J. R. Myra, D. A. D'Ippolito, S. I. Krasheninnikov, and G. Q. Yu, Phys. Plasmas **11**, 4267 (2004).
[15]D. A. D'Ippolito and J. R. Myra, Phys. Plasmas **9**, 3867 (2002).
[16]E. J. Strait, T. A. Casper, M. S. Chu *et al.*, Phys. Plasmas **4**, 1783 (1997).
[17]P. B. Snyder, H. R. Wilson, and A. W. Webster, "Toroidal flow shear effects on intermediate to high-n peeling-ballooning modes".
[18]M. Valovic, M. Edwards, D. Gates, S. J. Fielding, T. C. Hender, J. Hugill, A. W. Morris, and The COMPASS team, Proceedings of 21st EPS Conference, Montpelier, Part I, 1994.
[19]A. Kirk, H. R. Wilson, G. F. Counsell *et al.*, Phys. Rev. Lett. **92**, 245002-1 (2004).
[20]M. E. Fenstermacher, A. W. Leonard, T. H. Osborne *et al.*, "Structure, Stability and ELM Dynamics of the H-Mode Pedestal in DIII-D," Nucl. Fusion (submitted).
[21]J. A. Boedo, D. L. Rudakov, E. Hollman *et al.*, "Edge localized mode dynamics and transport in the scrape-off-layer of the DIII-D tokamak," Phys. Plasmas; J. A. Boedo, D. L. Rudakov, E. M. Hollmann *et al.*, "ELM-induced plasma transport in the DIII-D SOL," J. Nucl. Mater. **337**. 771 (2005).
[22]M. R. Wade, K. H. Burrell, J. T. Hogan, A. W. Leonard, T. H. Osborne, P. B. Snyder, and D. Coster, "Edge impurity dynamics during an ELM cycle on DIII-D," this conference, Phys. Plasmas (submitted).